The initial product vibrational energy distribution in the reaction between O(1 D 2) and H2

P. M. Aker and J. J. Sloan

Citation: The Journal of Chemical Physics **85**, 1412 (1986); doi: 10.1063/1.451230
View online: http://dx.doi.org/10.1063/1.451230
View Table of Contents: http://scitation.aip.org/content/aip/journal/jcp/85/3?ver=pdfcov
Published by the AIP Publishing

The initial product vibrational energy distribution in the reaction between $O(^1D_2)$ and H_2

P. M. Aker and J. J. Sloan
Division of Chemistry, National Research Council of Canada, 100 Sussex, Drive, Ottawa, Ontario, Canada K1A 0R6 and Department of Chemistry, Carleton University, Ottawa, Ontario, Canada K1S 5B6

(Received 20 February 1986; accepted 14 April 1986)

We report the first determination of the initial vibrational distribution in the OH product of the reaction between $O(^1D_2)$ and H_2. The measurement was made using a novel time-resolved Fourier transform spectroscopic technique which permits the observation of spectra on a microsecond time scale at a known time after the initiation of a reaction. The result is $P(v' = 1{:}2{:}3{:}4) = 0.29{:}0.32{:}0.25{:}0.13$ suggesting that the reaction dynamics involve very large attractive energy release during reagent approach followed by an extremely short-lived interaction leading to products within a few vibrational periods.

I. INTRODUCTION

We have previously reported[1] the first measurement of the complete vibrational distribution in the $OH(X\,^2\Pi)$ product of the reaction

$$O(^1D_2) + H_2 \rightarrow OH(X\,^2\Pi; v', J'). \quad (1)$$

The result of this measurement, reported as a lower limit to the correct initial vibrational distribution was $P(v' = 1{:}2{:}3{:}4) = 0.26{:}0.29{:}0.28{:}0.17$.

This result was reported as a lower limit because the technique used in Ref. 1 involved a quasi-steady-state measurement in which a conventional Fourier transform spectrometer was used to observe $OH(v')$ created in a pulsed-mode experiment. Such an experiment observes a weighted time average of the emission intensity. As a consequence of this and of the experimental conditions, it could not be guaranteed that the vibrational populations derived from these observations were free of collisional relaxation. In the following, we shall report a time-resolved measurement of this vibrational distribution which eliminates this difficulty by making the observation at a known (short) time after the creation of the $OH(v')$. In this latter measurement, we have obtained the initial vibrational distribution for reaction (1).

The $O(^1D_2)/H_2$ reaction has been the subject of intensive experimental study for many years. The rotational distributions in the OH $v' = 0$ and $v' = 1$ levels have been determined very accurately.[2–5] Recently, that in the $v' = 2$ level has been measured as well.[6] The rotational distributions are all broad and all exhibit inversion. Product angular distribution measurements obtained in molecular beam studies gave an early indication that the reaction may not be a simple, direct collisional abstraction.[7] The value of the isotopic branching ratio observed in the $O(^1D_2)$ + HD reaction also indicated that an HOD intermediate is probably involved.[8]

Extensive theoretical study of this system[9–21] has also been carried out, often in parallel with the experimental work. There have been several potential energy surface calculations,[9,10,13,14,17–20] each of which provides an accurate description in one part of the system's coordinate space. Straightforward energetic and kinematic considerations, some of which have been explored in dynamical calculations,[10–16,21] suggest that the reaction dynamics are most strongly influenced by a few important aspects of the potential energy surface, such as the location and magnitude of the energy barriers, the presence of the deep H_2O potential energy minimum and the existence of hyperconical intersections between the different potential energy surfaces which are energetically accessible to the reaction.

One of the most comprehensive surface calculations to date[18] reported a negligible energy barrier for the reaction in the C_{2v} configuration and a barrier of about 4 kcal mol^{-1} for the collinear reaction, thus enhancing the plausibility of the insertion mechanism suggested above. All of the calculations, of course, reproduce the extremely deep H_2O potential energy minimum. This minimum should have a profound influence on the dynamics because of the large impulse which it generates in regions of small reagent separation. The available information about the reaction, to be discussed in later sections, suggests that this aspect of the potential surface causes the $O(^1D_2)/H_2$ reaction to exhibit unique dynamical behavior. The distortions induced in the regions of Σ–Π hyperconical intersections (especially near the linear HHO an HOH configurations) have not been accurately represented for the purpose of the dynamical calculations, although these regions may be important to the outcome of the reaction.

Several of the dynamic calculations have reported very broad vibrational distributions which, in some cases, have population inversions between one or more of the vibrational levels.[13–16] It has been suggested[13,14] that this shape may be the sum of two distributions produced by reaction through two channels: insertion, which populates the lower vibrational levels, and abstraction, which produces a strongly inverted distribution.

The alternative suggestion—that the entire distribution may be due to the insertion process—has also been made.[15,21] The creation of an inverted vibrational distribution by a reaction forming an intermediate as strongly bound as H_2O has not been documented previously. Usually, the lifetime of such a strongly bound intermediate is long, with the result that the partitioning of the reaction exoergicity is completely random. In the case of the $O(^1D_2)/H_2$ reaction, however, the intermediate is very small and the unusual energetics and kinematics of this reaction, involving the possi-

 0021-9606/86/151412-06$02.10

ble formation of very strong bonds by two light atoms, make it plausible that the intermediate might have an extremely short lifetime. The experimental evidence to be presented in later sections of this paper supports this view.

The vibrational distribution obtained in this study is very broad, having approximately equal populations in the first three vibrational levels and a smaller population in the fourth. It resembles the result reported in Ref. 1 closely. This distribution, when combined with the rotational distributions measured elsewhere and the dynamical calculations described above, indicated that the reaction is neither a direct abstraction nor an insertion which forms a long-lived intermediate. Rather it is a "direct insertion" in which the lifetime of the (H–O–H) intermediate is very short. The existing data on this reaction are all consistent with a dynamical picture in which the favored approach of the $O(^1D_2)$ atom is laterally toward the H–H bond. The reaction proceeds via a very rapid insertion into this bond followed by the decomposition of the H–O–H intermediate within one (or a very few) bending vibrations. These dynamics may be thought of as the insertion analog of a simple "stripping" reaction. Although the insertion mechanism implies that the $O(^1D_2)$ atom must interact with both H atoms, the very strong forces which are released and the very small reduced masses for both the reactive collision and the product separation cause this interaction to be extremely brief. This inhibits the loss of the reaction exoergicity out of the newly formed bond, thus producing the same observable result as the dynamically simpler stripping reaction. In this sense, the dynamics of the $O(^1D_2)/H_2$ reaction appear to be unique.

II. EXPERIMENTAL

This experiment differs in one important aspect from any previously carried out on this system: we have used time-resolved Fourier transform spectroscopy to record the emission spectrum of the OH created in the reaction as a function of time after the $O(^1D_2)$ generation. The overall configuration of the experiment will be described first, then the time-resolved aspect will be outlined in more detail.

The large, high-throughput vacuum chamber and pumping system used in these experiments has been fully described in recent publications.[22–24] The reaction chamber is a 25 cm diam by 25 cm high stainless steel cylinder evacuated through a 31 cm diam gate valve by an 8000 ℓ/s diffusion pump. The O_3 and H_2 reagent are introduced through two concentric quartz tubes mounted in the reaction chamber lid and centered on the axis of the cylinder. Certain aspects of the reagent inlet geometry can be adjusted in order to localize the reagent mixing in a desirable part of the apparatus. The behavior of this reagent inlet has been accurately represented in a numerical model[23] and several internal checks, carried out in previous work,[24] demonstrate that it produces a well-defined, predictable reagent flow.

Immediately beneath the reagent inlet, the gas flow is intersected at right angles by a KrF excimer laser beam (Lumonics model TE-860T-4, operating at 330 Hz) which is multipassed through the reagent gases by two dielectric mirrors, coated for maximum reflectivity at 248 nm and mounted facing each other across the cylindrical chamber. At 248 nm, the O_3 photolysis produces $O(^1D_2)$ and $O_2(^1\Delta)$ with a 90% quantum efficiency. Following the photolysis, vibrationally and rotationally excited OH is formed promptly in collisions with H_2 (the reactive rate constant, 3×10^{-10} cm^3 $molecule^{-1}$ s^{-1},[25] is approximately gas kinetic). A Welsh cell, mounted with its axis perpendicular to both the axis of the laser-multipass mirrors and the gas flow, collects the infrared emission from the $OH(v', J')$ and focuses it out through an $f/1$ CaF_2 lens into a conventional Fourier transform spectrometer.

The time-resolved aspect of the experiment is accomplished by using an LSI11/23 processor to monitor the operation of the Fourier transform spectrometer and to time the O_3 photolysis synchronously with the data aquisition. This computer also controls certain amplifiers and/or electrical filters in the data channel. By observation of the clock signal derived from the interferogram of the reference laser in the Fourier transform spectrometer, the timing computer can predict (within ± 5 μs) the time at which the next data point on the signal interferogram will be digitized. At the requisite time before this data point, the timing computer triggers the excimer laser to initiate the reaction, then sets the bandwidth of the electrical filters and the gain of the data channel amplifier for the data aquisition. The data point is then digitized by the interferometer.

Since the minimum digitization rate of the Fourier transform spectrometer is higher than the maximum repetition rate of the excimer laser, it is not possible to have the infrared emission signal (from the reaction, which is initiated by the laser photolysis of O_3) present during the digitization of each data point. In order to eliminate the noise which would be introduced by co-adding the data points having no signal with those which contain signal, the bandwidth of the electrical filters and/or the gain of the data channel amplifier are set to zero while the "signal-off" data points are taken. A separate routine in the timing computer ensures that each

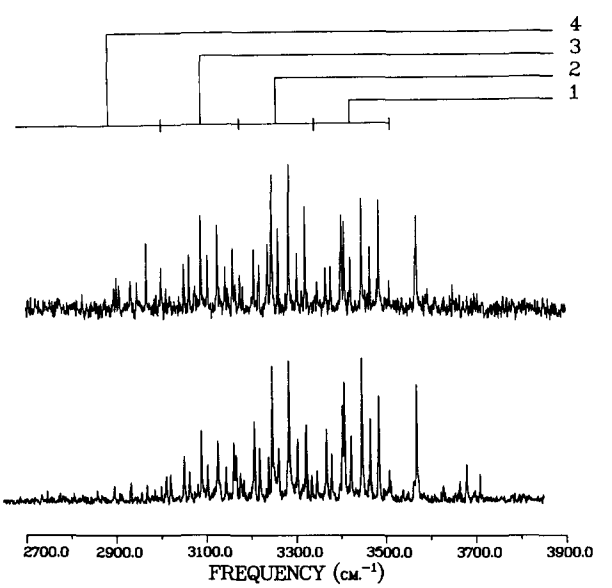

FIG. 1. Fundamental vibrational emission spectrum of OH observed under conditions of least (top) and most (bottom) vibrational deactivation (see Table I). The upper vibrational level of each observed transition is identified in the upper right hand corner; the location of the first four *P*-branch lines from each of these transitions is indicated across the top.

TABLE I. The experimental conditions and measured vibrational distributions. Collision No. is the number of gas kinetic collisions suffered by the OH product with each reagent, assuming a translational temperature of 300 K. $\langle Z_{eff} \rangle$ is the sum over both reagents of the collision number times an estimated "worst-case" probability for vibrational deactivation.

Concentration (10^{-3} Torr)		Delay	Collision No.			Vibrational populations			
$[H_2]$	$[O_3]$	(μs)	H_2	O_3	$\langle Z_{eff} \rangle$	$v'=1$	$v'=2$	$V'=3$	$V'=4$
11	15	40	16	8	1.8	0.32	0.35	0.22	0.11
9	24	40	13	13	2.9	0.28	0.31	0.25	0.16
1	19	80	3	22	4.8	0.28	0.31	0.28	0.13
75	75	50	141	53	11.7	0.33	0.32	0.21	0.14
10	26	150	56	55	12.2	0.34	0.30	0.23	0.13
75	75	190	536	202	44.6	0.45	0.29	0.19	0.07
50	90	400	752	512	112.8	0.51	0.29	0.15	0.05

data point in the signal interferogram receives the same amount of observation time. A single time-delay spectrum is obtained by Fourier transforming the sum of about 300 interferograms, each taken with the same value of the time-delay parameter.

The ozone used in these experiments is generated in a conventional silent-arc ac discharge operated at atmospheric pressure and -78 °C. The ozone is stored in a dry-ice-cooled silica gel trap under an atmosphere of oxygen. Just prior to use in an experiment, the oxygen is pumped away and the total pressure in the trap is (briefly) reduced below 5 Torr. Since the equilibrium vapor pressure of O_3 on silica gel is about 15 Torr, this precaution not only removes all of the oxygen, but some of the O_3 as well. A controlled O_3 flow of a few micromoles per second is admitted to the reagent inlet through Pyrex tubing by slow removal of the cooling medium during the experiment. The pressure in the reaction chamber, and hence the number of gas phase collisions during the delay time was set by adjusting the gate valve above the diffusion pump. The hydrogen was obtained from Air Products Co. and used without further purification.

III. RESULTS

In the time-resolved experiments reported here, $O(^1D_2)$ is formed only during the (approximately) 10 ns while the excimer laser irradiates the O_3. Since the $O(^1D_2)/H_2$ reaction rate is about 3×10^{-10} cm^3 molecule^{-1} s^{-1},[25] all of the $O(^1D_2)$ is removed and the $OH(v', J')$ product is formed within 1–2 gas kinetic collisions (about 10^{-5} s at the lowest pressures) following the irradiation. The rise of the infrared emission is limited by the finite electrical bandwidth of the signal channel to about 2×10^{-5} s. The minimum delay time used in this work is 4×10^{-5} s.

Figure 1 shows the $\Delta v' = -1$ fundamental OH emission observed under the conditions of least (top) and most (bottom) product vibrational deactivation. Both the rotational structure and the spin doublets are completely resolved. The quantum number of the upper vibrational level is given at the upper right hand corner and the approximate spectral location of the P-branch emission from each vibrational band is indicated at the top of the figure. These spectra show the quality of the data obtained using the time-resolved Fourier transform technique. The top spectrum has the poorest signal-to-noise used in this study. On this basis, the experimental uncertainty in the reported populations was estimated to be ± 0.03. These spectra show that there is intense emission from all thermodynamically accessible vibrational levels at the shortest delay time.

The results of time-resolved spectral measurements carried out at several combinations of reagent pressure and delay time are presented in Table I. The populations have been normalized such that $\Sigma_{v'=1}^{4} P(v') = 1.0$. (In the experiment, however, the observed populations decrease rapidly with time due to the removal of the emitters from the observation zone.) The data are given in terms of the total number of gas kinetic collisions (assuming thermal velocities at 300 K) which the OH suffers with each of the reagents during the time between photodissociation and spectral observation. The average effective collision number $\langle Z_{eff} \rangle$ is also given. This is the sum (over both reagents) of the total number of $OH(v', J')$/reagent collisions, times the average probability for deactivation in collisions with that reagent. The latter probability was estimated from reported rate constants for $OH(v'=9)$ removal by O_3 (2×10^{-10} cm^3 molecule^{-1} s^{-1} [26]) and by H_2 (1.7×10^{-13} cm^3 molecule^{-1} s^{-1}).[27,28] The average rates for the lower vibrational levels were obtained from the $v'=9$ rates using the vibrational dependence of the $OH(v')/O_3$ removal reported in Ref. 29. Although indirect, this procedure likely provides better than an order of magnitude estimate for $\langle Z_{eff} \rangle$, which in any event is dominated by the O_3 relaxation.

The quality of the data do not warrant attaching any significance to the differences among the distributions measured for the smallest three values of $\langle Z_{eff} \rangle$, all of which show a slight inversion in the $v'=2/v'=1$ population ratio. In these three runs, the major deactivator changes from H_2:O_3 = 2:1 to O_3:H_2 = 7:1. This represents a substantial change in the experimental conditions for deactivation and the invariance of the data (within the experimental uncertainty) indicates that no significant relaxation has taken place for these runs. Therefore, the average of these data—$P(v'=1{:}2{:}3{:}4) = 0.29{:}0.32{:}0.25{:}0.13$—represents the initial distribution created by the reaction.

The behavior of these populations as a function of the number of deactivating collisions $\langle Z_{eff} \rangle$ is shown in Fig. 2. The curve at the smallest value of $\langle Z_{eff} \rangle$ is the average of the

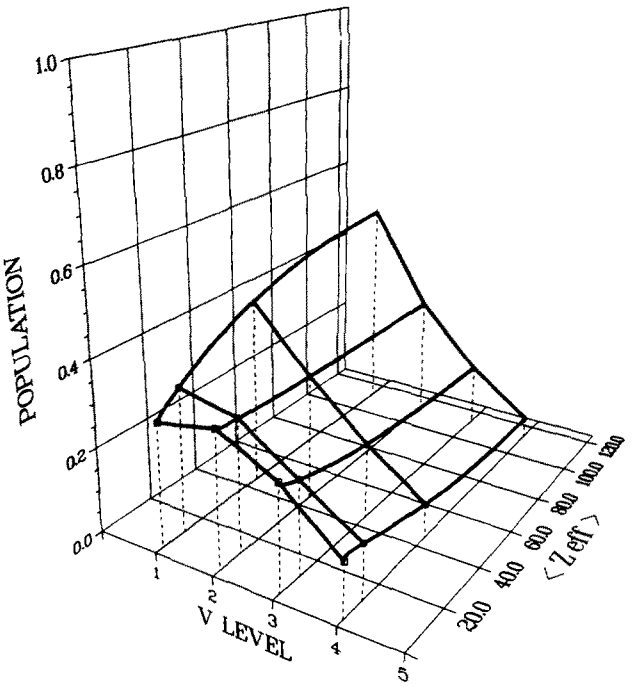

FIG. 2. The OH vibrational populations as a function of the average number of deactivating collisions which occur between the initiation of the reaction and the observation. The sum of the populations in each distribution is separately normalized to 1.0.

first three distributions in Table I; the next curve is the average of the fourth and fifth distributions. These curves show qualitatively that the populations of the upper vibrational levels decrease more quickly than those in the lower levels. The rate constants for collisional vibrational deactivation decrease with decreasing vibrational level[29] and thus the "cascading" relaxation process causes the transitory buildup of population in the lower levels before the eventual decay into $v' = 0$. These data, with an appropriate master equation model of the relaxation should permit the extraction of state-to-state energy transfer rate constants for this system. A much larger experimental data base will be required for this purpose, which will be the subject of a later publication.

IV. DISCUSSION

The OH energy distribution which can be constructed from the vibrational data reported here and the rotational distributions obtained elsewhere[2–6] is unusual in the context of this kind of reaction. This is best illustrated by comparison with the kinematically and kinetically similar $F + H_2$ reaction, which is known to proceed via simple, direct abstraction dynamics to produce rotationally and vibrationally inverted HF.[30–33] The total energy available to the products of the $F + H_2$ reaction is 148 kJ mol^{-1},[31] whereas the energy available to the OH from reaction (1) is 196 kJ mol^{-1} [including about 8 kJ mol^{-1} relative translational energy resulting from the fact that the photolysis creates the $O(^1D_2)$ atom with a translational energy of about 42 kJ mol^{-1} in the $O_2(^1\Delta)$–$O(^1D_2)$ frame of reference].

The HF rotational distribution from the $F + H_2$ reaction is broad and inverted[30,31] but the OH rotational distribution from the $O(^1D_2) + H_2$ reaction,[2,5,6] appears to be even more inverted. The vibrational distributions are also both inverted but the $F + H_2$ vibrational distribution [$P(v' = 1{:}2{:}3) = 0.15{:}0.55{:}0.30$[31]] is much more strongly peaked than the slightly inverted OH distribution [$P(v' = 1{:}2{:}3{:}4) = 0.29{:}0.32{:}0.25{:}0.13$] which we report here.

Extensive comparison between the measured $F + H_2$ product energy distributions and dynamical calculations on accurate potential energy surfaces (see Ref. 33 and references therein) have shown that the specificity implied by the strong vibrational peaking is the result of single-collision reaction dynamics on a strongly repulsive potential energy surface favoring collinear approach. The $O(^1D_2)/H_2$ potential surface differs from this in two major ways. First, it has a high (16–20 kJ mol^{-1}) energy barrier to collinear approach[18] and a very small (or zero) barrier for C_{2v} approach[12,14,18] while the relative heights of these barriers are reversed on the F/H_2 surface. As a result of this, the dynamical calculations on the $O(^1D_2)/H_2$ system have found that the C_{2v} insertion mechanism predominates and those on the F/H_2 surface have found that collinear abstraction is most important.

The second significant difference is the deep H_2O potential well in the $O(^1D_2)/H_2$ surface which has no counterpart in the smoothly repulsive F/H_2 surface. The definitions which characterize the attractive or repulsive nature of potential energy surfaces[34] do not strictly apply to the $O(^1D_2)/H_2$ insertion topography but it is clear nevertheless that the H_2O potential energy well strongly increases the attractive character of the $O(^1D_2)/H_2$ surface.

The shapes of the observed energy distributions are consistent with the suggestion that the relative heights of the barriers to reagent approach and the presence of the deep H_2O potential well dominate the dynamics of the $O(^1D_2)/H_2$ reaction. The energy barriers ensure that the majority of successful reactions (for modest translational energies) have their initial approach via the C_{2v} geometry. As the reagents reach the region of close approach in this geometry, the very steep slope of the H_2O potential well delivers an extremely strong impulse in the direction of the reaction coordinate [insertion of the $O(^1D_2)$ atom between the H atoms] causing very rapid motion of the system through the HOH configuration.

This unusually strong impulse appears to be crucial to the shape of the resulting OH vibrational distribution. In many previous studies of reactions involving strongly bound intermediates,[35–41] we have found that the vibrational populations of the diatomic product decrease monotonically with vibrational level, due to the statistical redistribution of the reaction exoergicity during the lifetime of the intermediate. (It can be shown that it is impossible to obtain an inverted vibrational distribution if the lifetime of the intermediate is long with respect to the time requried for energy randomization.) If the majority of the reaction occurs via insertion to form H_2O the slightly inverted $OH(v')$ distribution which we have observed therefore requries that the lifetime of this (very strongly bound) intermediate be much shorter than the time required for the randomization of the reaction energy.

Evidence that this is indeed the case has been obtained

from dynamical calculations, both in our laboratory and elsewhere.[35,36] These show that the combination of the strong impulse and the small reduced mass of the collision results in a very rapid passage through the bound HOH intermediate structure and into the product channel in one (or at most a few) vibrations of the HOH intermediate. This time scale is the same as that of the F + H_2 (direct) abstraction reaction, which occurs in about one or two vibrations of the H_2 reagent.[33] During this very brief interaction, there is not enough time for the intramolecular vibrational energy transfer which is necessary to distribute the reaction exoergicity completely among all the product modes. Thus the inversion in the $O(^1D_2)/H_2$ vibrational distribution is a consequence of the extremely curtailed interaction time; its greater breadth, in comparison to the F + H_2 distribution, results from the transitory participation of the third atom in the bonding of the H_2O intermediate.

In order to qualitatively illustrate this mechanism, we have made a contour plot (Fig. 3) of two sections through the $O(^1D_2)/H_2$ potential energy hypersurface. The surface used in this plot is based on the calculations of Howard *et al.*[10]; the contours are separated by 1.0 eV. The figure is intended to represent the potential energy changes which occur in a reaction having an idealized rectilinear reaction coordinate in which an $O(^1D_2)$ atom approaches the H–H bond in a C_{2v} configuration (sketched at the top of the figure), inserts to form linear, symmetrical HOH, then one of the H atoms is *collinearly* removed from the linear HOH. A diagonal line divides the figure into two halves; the upper left part is the potential energy surface for HOH in all C_{2v} configurations (hence the reagent approach coordinate for the idealized reaction) and the part at the lower right is the potential energy surface for collinear asymmetrical HO–H (hence the product separation coordinate). The diagonal line itself thus represents all linear *symmetrical* H–O–H configurations.

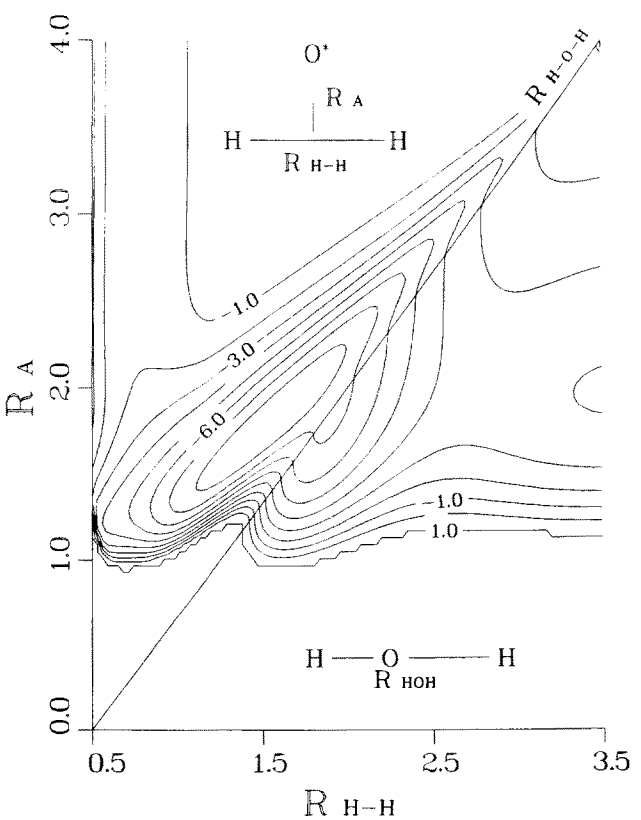

FIG. 3. Contour plot of two sections through the potential energy surface appropriate to an idealized rectilinear insertion reaction. The upper left part shows the insertion of $O(^1D_2)$ into H–H to form linear H–O–H. The lower right part shows the removal of one H atom from linear H–O–H.

The necessity to present these two potential energy maps together requires their distortion from the rectangular plots which are normally used, into triangular forms. The distortion was achieved in the upper half of the figure by scaling R_A [the perpendicular distance from the $O(^1D_2)$ atom to the center of the H–H bond] such that it always reaches zero at the location of the diagonal line. The distance between the H atoms in linear asymmetrical HO–H (described by the lower right part of the figure) is given by R_{H-H}—the scale shown at the bottom. The H–H distance for the linear symmetrical H–O–H may be obtained by projecting the scale on the R_{H-H} axis vertically upward until it intersects the diagonal line, which forms the common axis for the two halves of the figure.

From the above, it is clear that motion vertically along the R_A axis represents the reagent approach part of the reaction coordinate. Since all linear, symmetrical configurations occur on the diagonal line and both O–H distances increase at the same rate with increasing (diagonal) distance from the origin, motion along this line corresponds to the symmetrical stretching mode of linear H_2O. Motion to the right along any horizontal line in the lower part of the figure corresponds to the collinear removal of one H atom from the symmetrical H–O–H configuration defined by the intersection of that horizontal line with the diagonal axis. The initial H–H separation in the linear H–O–H is obtained by projecting this intersection point downward to the horizontal axis; each initial O–H distance is one-half of this value. In moving horizontally to the right in the lower half of the figure, one O–H distance remains fixed at this initial value while the other O–H distance is increased. This motion corresponds, therefore, to the antisymmetric stretching of linear H–O–H.

In this idealized representation, the entry valley for the reaction (at the upper left corner) is relatively flat until R_A is approximately 2 Å; then the potential energy begins to decrease very rapidly as the deep H–O–H potential well is encountered. As the system enters this region, strongly attractive forces draw it toward the bottom of the H_2O potential well and the sharp curvature of the minimum energy path deflects it into a direction approximately parallel to the diagonal line. In the reaction, this process represents the release of attractive energy as the $O(^1D_2)$ atom inserts into the H_2 bond and collides with both of the H atoms, driving them apart and thereby exciting the H_2 symmetric stretching vibration. This first (hard) O–H_2 collision is primarily responsible for creating the initial vibrational excitation in the H_2O intermediate which subsequently becomes vibration in the OH product.

Motion of the system in the lower right part of the countour plot can be decomposed into the components of the symmetric and antisymmetric vibrations as described above.

Motion along the diagonal corresponds to the purely symmetric vibration, horizontal motion to the antisymmetric. The strong impulse and the sharp curvature of the minimum energy path propels the system into a trajectory roughly parallel with the diagonal (symmetric vibration). Thereafter, anharmonic coupling between the symmetric and antisymmetric vibrations causes the excitation of the latter in a way which cannot be represented in a classical picture such as that given by the contour plot. The result can be visualized, however, as the progress of the system out the exit valley toward the right with an oscillatory motion corresponding to the (classical) combination of the symmetric and antisymmetric vibrations.

V. CONCLUSION

Using a novel time-resolved Fourier transform spectroscopic technique, we have made the first determination of the initial vibrational distribution from the reaction of $O(^1D_2)$ atoms with H_2 molecules. The vibrational distribution is broad and slightly inverted. The product energy distribution constructed from this result and the rotational distribution observed in other laboratories is consistent with a very short-lived insertion reaction in which the product separation occurs within one or a few vibrations of the resulting H_2O intermediate. Such dynamics, while unusual, are plausible in view of the small reduced masses and strong forces involved in the reaction.

ACKNOWLEDGMENTS

The authors are pleased to acknowledge helpful discussions of their results, prior to publication, with Dr. P. J. Kuntz, Dr. J. T. Muckerman, and Professor G. C. Schatz.

[1]J. E. Butler, R. Glen Macdonald, D. J. Donaldson, and J. J. Sloan, Chem. Phys. Lett. **95**, 183 (1983).
[2]A. C. Luntz, R. Schinke, W. A. Lester, Jr., and Hs. H. Gunthard, J. Chem. Phys. **70**, 5908 (1979).
[3]G. K. Smith, J. E. Butler, and M. C. Lin, Chem. Phys. Lett. **65**, 115 (1979).
[4]A. C. Luntz, J. Chem. Phys. **73**, 1144 (1980).
[5]G. K. Smith and J. E. Butler, J. Chem. Phys. **73**, 2243 (1980).
[6]G. M. Jurisch and J. R. Wiesenfeld, Chem. Phys. Lett. **119**, 511 (1985).
[7]R. Buss, P. Casavecchia, T. Hirooka, S. J. Sibener, and Y. T. Lee, Chem. Phys. Lett. **82**, 386 (1981).
[8]K. Tsukiyama, B. Katz, and R. Bersohn, J. Chem. Phys. **83**, 2889 (1985).
[9]K. S. Sorbie and J. N. Murrell, Mol. Phys. **29**, 1387 (1975); **31**, 905 (1976).
[10]R. E. Howard, A. E. Maclean, and W. A. Lester, Jr., J. Chem. Phys. **71**, 2412 (1979).
[11]R. Schinke and W. A. Lester, Jr., J. Chem. Phys. **70**, 4893 (1979).
[12]R. Schinke and W. A. Lester, Jr., J. Chem. Phys. **72**, 3754 (1980).
[13]P. A. Whitlock, J. T. Muckerman, and P. M. Kroger, in *Potential Energy Surfaces and Dynamics Calculations*, edited by D. G. Truhlar (Plenum, New York, 1981).
[14]P. A. Whitlock, J. T. Muckerman, and E. R. Fisher, J. Chem. Phys. **76**, 4468 (1982).
[15]S. W. Ransome and J. W. Wright, J. Chem. Phys. **77**, 6346 (1982).
[16]L. J. Dunne and J. N. Murrell, Mol. Phys. **50**, 635 (1983).
[17]J. N. Murrell and S. Carter, J. Phys. Chem. **88**, 4887 (1984).
[18]G. Durand and X. Chapuisat, Chem. Phys. **96**, 381 (1985).
[19]R. Polák, I. Paidarová, and P. J. Kuntz, J. Chem. Phys. **82**, 2352 (1985).
[20]P. J. Kuntz and R. Polák, Chem. Phys. **99**, 405 (1985).
[21]G. C. Schatz (private communication).
[22]D. J. Donaldson and J. J. Sloan, J. Chem. Phys. **82**, 1873 (1985).
[23]D. J. Donaldson, J. D. Goddard, and J. J. Sloan, J. Chem. Phys. **82**, 4524 (1985).
[24]P. M. Aker, D. J. Donaldson, and J. J. Sloan, J. Phys. Chem. (accepted).
[25]G. Paraskevopoulos and R. J. Cvetanovic, J. Am. Chem. Soc. **91**, 757 (1969).
[26]G. D. Greenblatt and J. R. Wiesenfeld, J. Geophys. Res. **87**, 11, 145 (1982).
[27]B. J. Finlayson-Pitts, D. W. Toohey, and M. J. Ezell, Int. J. Chem. Kinet. **15**, 151 (1983).
[28]O. Kajimoto, Y. Tanaka, K. Tadatomo, and T. Fueno, in *Proceedings of Yamada Conference III on Free Radicals*, edited by Y. Morino, I. Tanaka, E. Hirota, K. Obi, and S. Saito (Association for Science Documents Information, Japan, 1983).
[29]R. N. Coltharp, D. S. Worley, and A. E. Potter, Appl. Opt. **10**, 1786 (1971).
[30]J. C. Polanyi and K. B. Woodall, J. Chem. Phys. **57**, 1574 (1972).
[31]D. S. Perry and J. C. Polanyi, Chem. Phys. **12**, 419 (1976).
[32]D. J. Douglas and J. C. Polanyi, Chem. Phys. **16**, 1 (1976).
[33]J. C. Polanyi and J. L. Schreiber, Faraday Discuss. Chem. Soc. **62**, 267 (1977).
[34]J. C. Polanyi, Acc. Chem. Res. **5**, 161 (1972).
[35]R. G. Macdonald and J. J. Sloan, Chem. Phys. **31**, 165 (1978).
[36]R. G. Macdonald and J. J. Sloan, Chem. Phys. **40**, 201 (1979).
[37]D. J. Douglas and J. J. Sloan, Chem. Phys. **46**, 307 (1980).
[38]J. J. Sloan and D. G. Watson, J. Chem. Phys. **74**, 744 (1981).
[39]D. J. Donaldson, J. J. Sloan, and D. G. Watson, Chem. Phys. **68**, 95 (1982).
[40]D. J. Donaldson and J. J. Sloan, J. Chem. Phys. **82**, 1873 (1985).
[41]D. J. Donaldson, J. D. Goddard, and J. J. Sloan, J. Chem. Phys. **82**, 4524 (1985).
[42]P. M. Aker, J. J. Sloan, and J. S. Wright (to be published).
[43]J. T. Muckerman (private communication).